

Core-to-Specimen Energy Coupling Results of the First Modern Fueled Experiments in TREAT

Nicolas Woolstenhulme – ORCID: 0000-0002-7881-3314 – Nicolas.Woolstenhulme@inl.gov

Austin Fleming – ORCID: 0000-0002-6801-5028 – Austin.Fleming@inl.gov

Tommy Holschuh – ORCID: 0000-0002-1521-4314 – Tommy.Holschuh@inl.gov

Colby Jensen – ORCID: 0000-0001-8925-7758 – Colby.Jensen@inl.gov

David Kamerman – ORCID: 0000-0002-2610-038X – David.Kamerman@inl.gov

Dan Wachs – ORCID: 0000-0002-9239-3424 – Daniel.Wachs@inl.gov

Idaho National Laboratory, 2525 N. Fremont Ave, Idaho Falls, Idaho 83415

Corresponding Author:

Nicolas Woolstenhulme

Idaho National Laboratory, 2525 N. Fremont Ave,

P.O. Box 1625, MS 3855, Idaho Falls, Idaho 83415

Phone: (208) 526-1412, Email: Nicolas.Woolstenhulme@INL.gov

Abstract – The Transient Reactor Test Facility (TREAT) is a unique graphite-based test reactor residing at the Idaho National Laboratory. TREAT was first constructed in the late 1950's to support research on nuclear fuel specimens under extreme nuclear-heated conditions. This work continued in various forms until 1994 when reactor operations were suspended. Following a decades-long hiatus and subsequent refurbishment of the facility, reactor operations were resumed at TREAT in 2017 to support the reemerging field of fuel safety research. A series of physics tests were then performed to acquaint a new team of operators and test designers with the facility's transient capabilities. These tests emphasized previously-undemonstrated transient categories with relevance for Light Water Reactor (LWR) fuels research. The successful outcome of these efforts enabled the first series of fueled-experiments to be conducted in TREAT since its restart. These fueled tests made use of fresh LWR-type sub-length specimens (4.9% enriched UO_2 in zirconium alloy cladding) in inert gas capsules with the primary objective to quantify the ratio of nuclear heat deposited in the core to that deposited in the specimens for a given transient. Several new experimental systems and processes were successfully commissioned and the desired energy coupling data were obtained. Five capsules were irradiated and energy coupling factors ranging from 2.0 to 2.2 $\text{J/gUO}_2\text{MJ}$ were observed over a wide range of transient energies with good agreement between in-situ calorimetric methods based on temperature measurement, post-test gamma spectroscopy, and observations of fuel behavior. Corroboration between these sources provided confidence in the measured values and supported the conclusion that the data should be used for calibrating models used in design and interpretation of future TREAT irradiation experiments.

Keywords – Nuclear Fuel Safety Research, Irradiation Testing, In-Pile Instrumentation, Irradiation Environment, Nuclear Testing, Transient Testing

I. Introduction

TREAT was constructed in the late 1950's, first achieving criticality in 1959, to support nuclear-heated safety testing for then-emerging fuel technologies. The facility was upgraded and reconfigured several times over the years, but always operated on the same basic principles. These principles employed a graphite-based core containing a dilute dispersion of uranium oxide fuel particles to serve as the neutron moderator and transient heat-sink [1] where the resulting negative temperature feedback behavior worked in concert with transient control rod systems to enable shaping of various power excursions such as prompt pulses, power ramps, and decay curves [2]. TREAT was refurbished and reactor operations resumed in 2017 in order to support fuel safety research for the US department of energy's Accident Tolerant Fuels (ATF) program as well as other fuel development data needs.

Post transient cooling in TREAT is hastened by an air blower system and the core is shielded by above-grade concrete, both of which enable a facility layout where it is straightforward to install new experiment devices into the core through slots in the top shield plug. While this arrangement does not easily permit facility-based semi-permanent experiment containment systems, it allows for relatively rapid transition between experiment types by using compact drop-in type capsules and loops having various coolant mediums within. These experiment packages can be handled outside the core using purpose-built shielded casks when needed. This strategy requires some unique approaches to experiment device engineering in order to support the specimens' boundary conditions, accommodate in-situ instrumentation, and safely contain any hazards [3].

II. Transient Prescription Studies

Just prior to suspension of reactor operations at TREAT in 1994 the facility was reconfigured with an upgraded transient and control rod drive system with corresponding core layout. At this

time a neutronic mockup of historic sodium loops was placed in the core (referred to as M8-CAL [4]) and reactor operations were performed to characterize steady state power coupling with representative specimens in the mock loop. Fissile dosimeter wires were employed to quantify differences in power coupling between transient and steady state irradiations.

The M8-CAL campaign relied on evaluation of fissile dosimeter samples to infer fission events and corresponding power coupling data. Fissile dosimeters did not gather real time nuclear heating data, but was a standard practice suitable to enable refined transient tuning and to obtain safety permission for final fueled transients. Since the M8-CAL core load was the existing mechanical configuration during TREAT's recent refurbishment, in addition to having been well characterized just prior to TREAT's hiatus, it was the core arrangement of choice for first operations in 2017. Transient shapes associated with core feedback characterization (i.e. temperature-limited pulses) and Sodium Fast Reactor (SFR) safety research (i.e. power ramps) were performed during this time to connect modern operations with historic data.

Prediction of transient specimen power coupling by computational methods was limited in TREAT's early history and, despite some advances in computational science, still proved evasive in its latter history due to complicated neutronic spatial/spectral transient effects [5]. This empirical approach to determining specimen power coupling continued to be mandatory following TREAT's restart in 2017 owing to the paramount importance of specimen nuclear heating in transient experiment design and safety analysis. An effort was undertaken to produce modern transient power coupling data following completion of the formal restart plan in early 2018, which focused on demonstrating transient shapes with relevance to LWR safety research which, owing to TREAT's almost exclusive emphasis on SFR research in its more recent historic era, transient relevant to LWR safety research had not been performed in the M8-CAL or similar large core

configurations. The objectives of this effort were to familiarize a new generation of experimenters and operators with the reactor, to demonstrate LWR transient capabilities in support of ATF/LWR research, and to begin gathering new data sources for modern model comparison and benchmarking. The latter of these objectives was also expected to be a common theme in future TREAT experimentation since tremendous advances in modern computational science were viewed with optimism for their potential to improve transient power coupling predictive capabilities.

The initial efforts were designed to be “physics tests,” in which nuclear fuel specimens are not tested in transient irradiations. The existing M8-CAL test vehicle was constructed primarily from stainless steel (giving it a reactivity worth comparable to most envisioned TREAT experiment vehicles for LWR research). As a result, the M8-CAL core was used for initial physics testing. The LWR-focused transients campaign addressed two main categories of LWR design basis accidents, including Reactivity Initiated Accidents (RIA) and Loss of Coolant Accidents (LOCA).

The LWR RIA category of design basis accidents are typically postulated to occur due to unintentional and rapid removal of neutron-poisoning control elements from the core, resulting in a rapid power excursion terminated by negative feedback physics. Due to differences in neutron lifetime between TREAT’s graphite-moderated core and a hydrogen-moderated LWR core, the innate pulse width in TREAT is longer than ideal for simulating pellet-cladding thermo-mechanical interactions in the narrowest postulated RIA pulses. TREAT can, however, approximate LWR RIA pulse widths by initiation from very lower core power on large step insertions of reactivity followed by rapid reinsertion of transient rods to “clip” the resulting pulse. Since the millisecond timing of the clipping action heavily influences core energy release, a series of three nominally identical pulses were performed to determine repeatability of the transient rod

electro-mechanical drive systems. The clipping repeatability tests demonstrated remarkably consistent behavior with less than 1% variation between tests on the most critical parameters of pulse width and core energy release. A series of companion irradiations were also performed which released the same amount of core energy through low power steady state and unclipped natural pulses. One irradiation from each of these three operation types included flux wires and depleted uranium fission wires for data comparison via gamma spectroscopy. Despite using depleted uranium, there was enough ^{235}U remaining in the depleted uranium wires that transient energy still had to be limited to approximately 30% of TREAT's full capacity to prevent their melting. The results of the dosimeter analysis and comparison to model results can be found in [6].

Then, without the fission wires to limit core energy release, a series of pulses were performed starting with very large step insertions of reactivity ($4.2\% \Delta k/k$) to achieve narrower pulses. Clip timing was varied between runs to determine TREAT's minimum pulse width. The minimum pulse width, measured as full width at half maximum (FWHM) of the M8-CAL half-slotted core configuration was found to be 89 ms; the narrowest pulse achieved in TREAT to date. The physics demonstrated in these tests gave rise to ongoing engineering efforts aimed towards special core configurations which will permit TREAT to achieve pulse widths representing boiling water reactor rod drop accidents (~ 75 ms) in the very near term. The data from this effort also enabled calibration of kinetic models and resulting design efforts of future enhanced clipping systems which predict that TREAT can achieve pulse widths representing hot zero power rod ejections in pressurized water reactors (PWR) at ~ 45 ms FWHM [7]. Transient power histories from these narrow pulse width transients can be seen in Figure 1 for transient operations 2904 through 2908. Each transient was performed with a pre-determined time for the transient rods to be reinserted following their full withdrawal from the core.

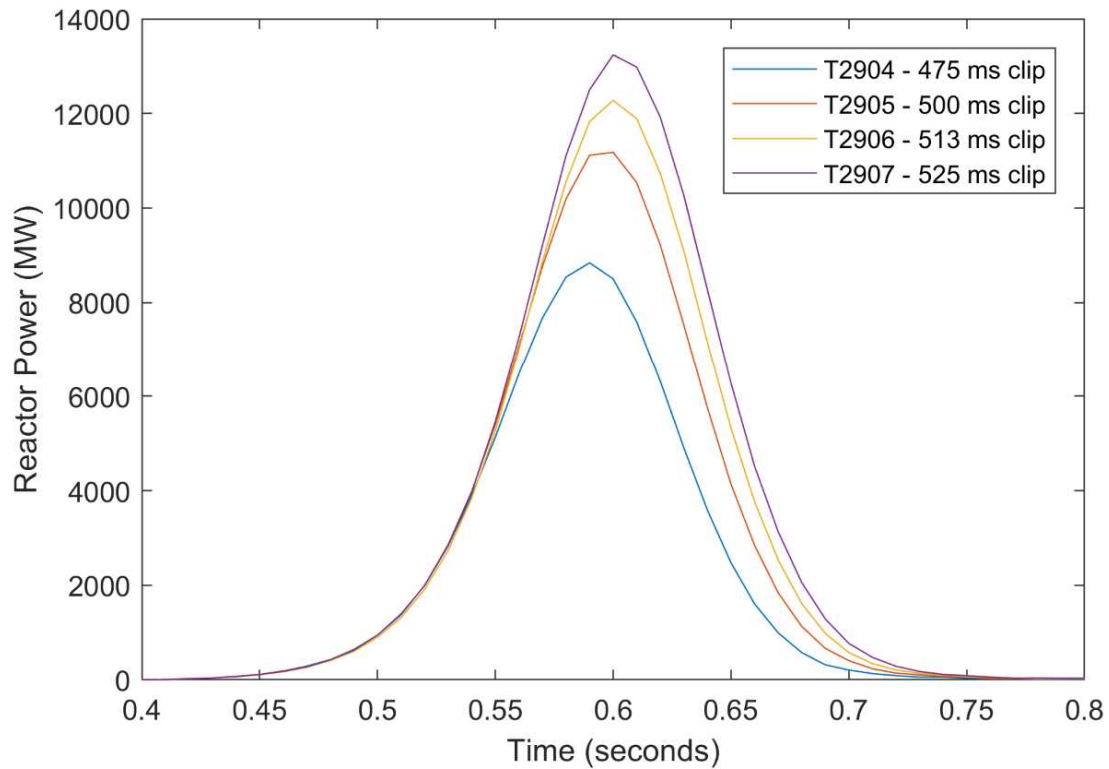


Figure 1: Narrow Pulse Width Transient Power Histories

Unlike RIAs, LOCAs are postulated to occur starting from normal power operations at full system pressure followed by a major breach of the primary coolant system pressure boundary. Such an event then results in rapid depressurization so that water changes to steam roughly coincident with a reactor shutdown (via SCRAM and/or loss of moderator). Fuel rods surrounded by steam then experience a long period of fuel rod overheating due to decay heat before liquid water re-enters the core and quenches the fuel. TREAT-based LOCA transients can be designed to simulate these conditions with an initial flattop transient for tens of seconds to develop representative temperature distributions in the fuel specimens, followed by a sizeable power reduction to a longer segment where low-level specimen fission heating represents internal decay heat generation. In future experiments, the designs of which are currently underway, capsules and

loops will synchronize depressurization and reflood actions with transient power shaping to simulate the full thermal-hydraulic evolution of LOCAs.

The objective of the LOCA transients performed in TREAT was markedly different than the RIA transients in essentially demonstrating the *longest* duration shaped transients possible in TREAT. Monte Carlo neutronics calculations were used to predict power coupling for high burnup LWR specimens (70 MWD/kgU) surrounded first by liquid water, and later by steam, in order to determine the appropriate power history for TREAT to simulate full prototypic nuclear heating in a LOCA. Two nominally identical transients were performed and showed superb repeatability. These transients showed that, with a 30 second preheat segment to represent pre-LOCA steady state conditions, TREAT can provide ~200 seconds of prototypic heating in the decay phase before the transient rods have been fully withdrawn and the core's negative temperature feedback reduces power to sub-megawatt levels. Reinsertion of transient control rods can be used to terminate the transient at any power, or the

This duration is significantly longer than the steam phase of typical postulated design-basis LOCA's, and could be clipped at any point, but is important in demonstrating that TREAT can provide headroom for simulating beyond-design-basis LOCA scenarios and margin quantification for potential LOCA-resistant fuels such as ATF designs. Transient power histories from these LOCA transients can be seen in Figure 2.

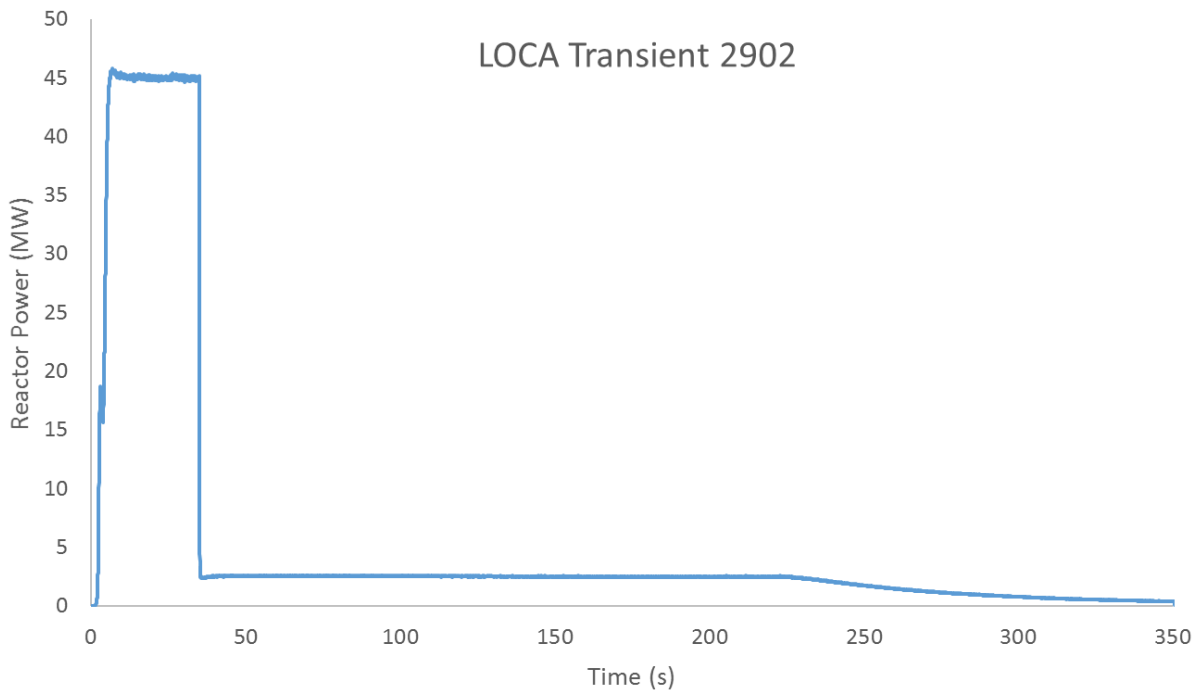


Figure 2: LOCA Transient Power History

III. Design of the First Modern Fuel Experiments

The previously-described transient demonstrations effectively commissioned TREAT as a neutron source for LWR fuel safety research. Following this effort the first fueled irradiation tests were performed to commission experimental systems and help gather specimen nuclear heating data. The first modern fueled irradiation device used in TREAT was developed to support high throughput testing and post transient examination by using relatively small fuel samples arranged in extractable experiment modules referred to as the Minimal Activation Retrievable Capsule Holder (MARCH). The MARCH system is composed of a nuclear-grade stainless steel containment pipe weldment which ensures that any hazards associated with transient testing are safely contained. Thermal insulation, a secondary sheet metal enclosure, an optional electric heater module, and reconfigurable data acquisition and control systems all work together to support

MARCH-based experiments within TREAT's core and enable rapid innovation cycles in experiment designs. For fuel specimen testing, these modules typically take the form of capsules filled with the desired environment (inert gas, water, liquid sodium, etc.). A more detailed design description and analytic characterization of the nuclear environment in the MARCH system can be found in [8] and [9], respectively.

The first fuel-bearing transient irradiation experiments to be performed in the recently-restarted TREAT were sponsored by the ATF program using capsule-type modules in the MARCH system. The capsule design, termed the Separate Effect Test Holder (SETH), included a 10-pellet sub-length rod (hereafter referred to as a "rodlet") of 4.9% enriched fresh fuel UO_2 pellets in zirconium alloy cladding having typical pressurized water reactor radial dimensions. Five of these capsules were constructed, each containing 1 atmosphere helium and four 1 mm diameter titanium-sheathed type K thermocouples (TC) welded to the specimen cladding surface. The first of these capsules (SETH-A) was unique with thermal insulation surrounding the rodlet. The insulation was composed of low-density microporous silica selected for its low thermal conductivity and low thermal neutron capture cross section. The junctions in all four TCs in SETH-A were ungrounded with the junction packed in high thermal conductivity diamond powder for increased response time. The TCs were oriented so that the sheath tip and junction area were normal to the cladding surface and welded using an autogenous micro tungsten arc weld to minimize thermal mass. The fragile nature of these welds gave concern that they could detach during capsule handling prior to irradiation. To address this concern, the bottom TC in SETH-A was welded like the others and then intentionally detached so that its response could be compared to the others to determine whether they remained attached. All TCs were arranged in a line along the central 6-pellet axial span of the rodlet since the end pellets were expected to exhibit lower temperature from heat loss

through the rodlet ends. The as-fabricated location of SETH-A's TCs is shown in Figure 3. The TCs are numbered from bottom to top as TC1 through TC4.

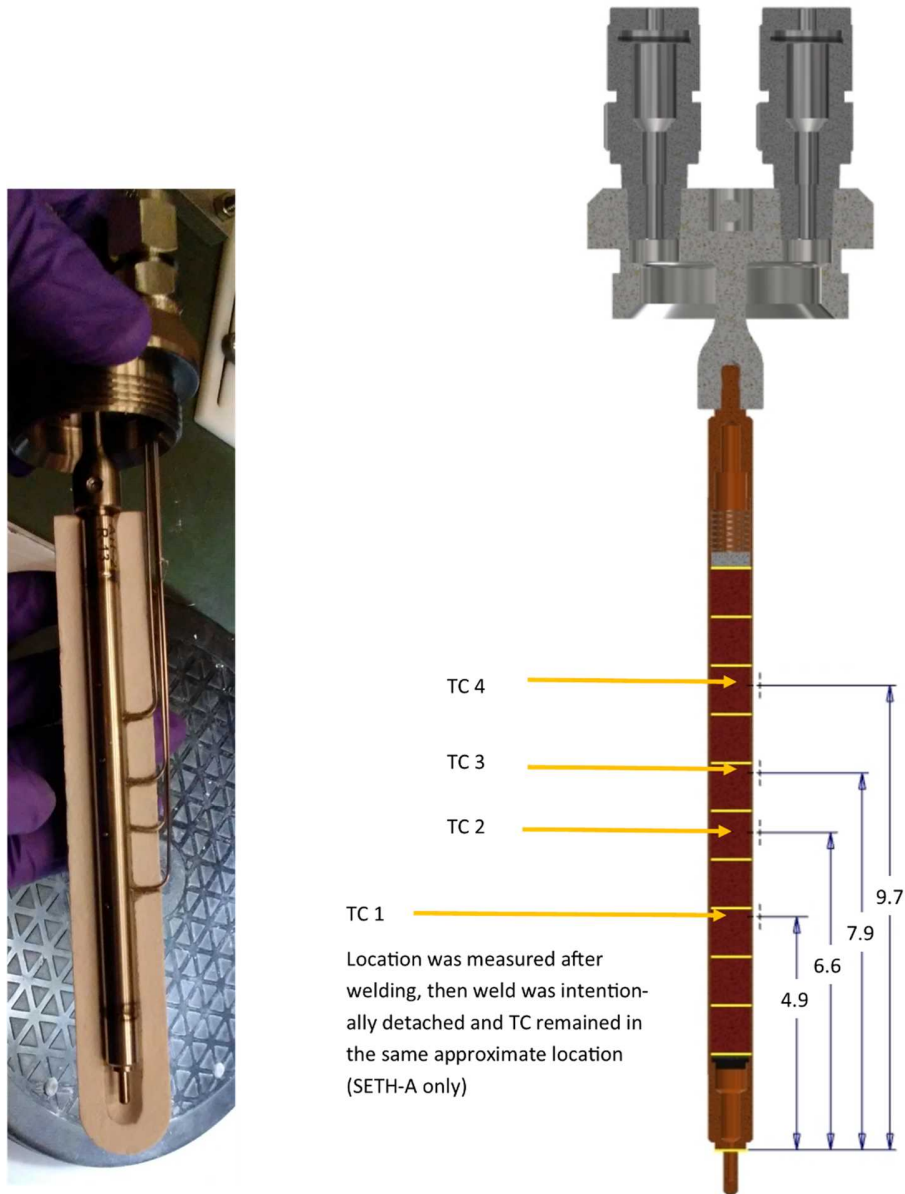


Figure 3: SETH-A Photo (left, one half of insulation removed) and TC Locations from Bottom End Cap, Dimensions in cm (right)

The TCs in the other four capsules (SETH-B through -E) were placed at the same nominal axial locations as SETH-A. TC1 and TC3 were the same diamond-packed type used in SETH-A

while TC2 and TC4 were nearly identical, except that their junctions were grounded to compare both their response time and noise sensitivity to noise in a newly constructed data acquisition system at TREAT. The SETH-B through -E rodlets were not surrounded by thermal insulation, but were instead encompassed by an aluminum cage designed to support instrumentation. These capsules were outfitted with a first-of-a-kind application for optical infrared multispectral pyrometry to determine whether this new technology, which was not used during TREAT's historic era, was well suited to providing fast-response, non-contact temperature measurements in a transient nuclear environment. The aluminum cage supported two silica optical fibers which were cleaved at an angle, polished, and aligned so that they were focused on the same area of the cladding surface, on the opposite side of the line of TCs, at approximately the axial center of the rodlet's fueled region. Both fibers were connected to identical multispectral pyrometers at TREAT to account for surface emissivity effects in real time. An image of the SETH-B through -E rodlet/instrumentation package can be seen in Figure 4.

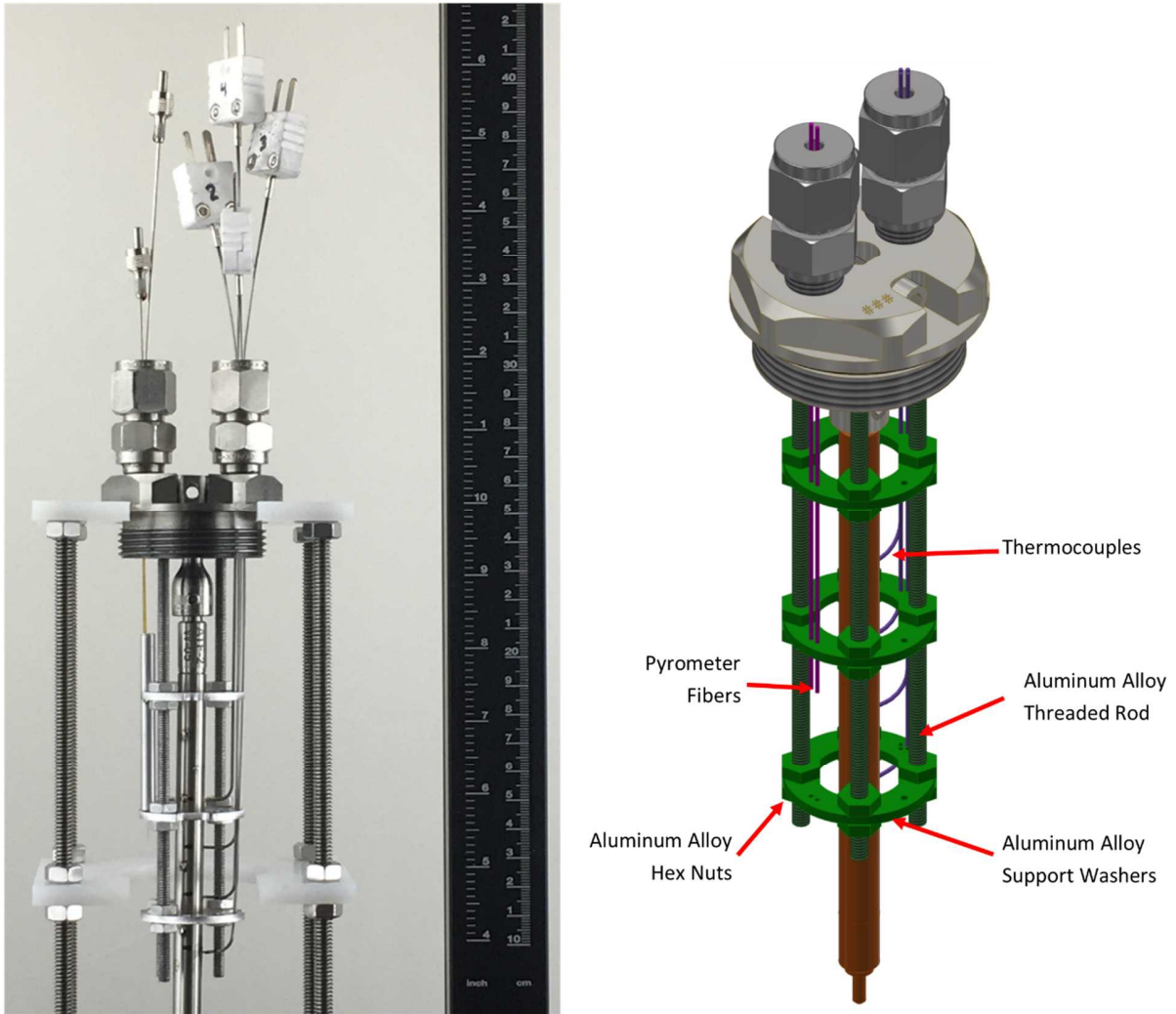


Figure 4: Images of SETH-B through -E Specimen, Instrument, and Assembly Photograph (left) and Design Rendering (right)

All SETH capsules were constructed from grade 5 titanium alloy owing to its adequate mechanical properties and constituents which would not remain significantly radioactive after brief neutron irradiations in TREAT. The first two SETH capsules (SETH-A and -B) were machined from titanium alloy barstock while the remaining three (SETH-C through -E) were manufactured by direct metal laser sintering followed by post machining on mechanical sealing surfaces. This advanced manufacturing method was not known to have been used in irradiation test capsule

applications previously, but its role in more affordably creating the mostly-hollow capsule geometry made the SETH capsule an ideal first application. All capsules contained two nested mullite ceramic crucibles to protect from potential molten fuel material. Images of the SETH capsule assembly are shown in Figure 5.

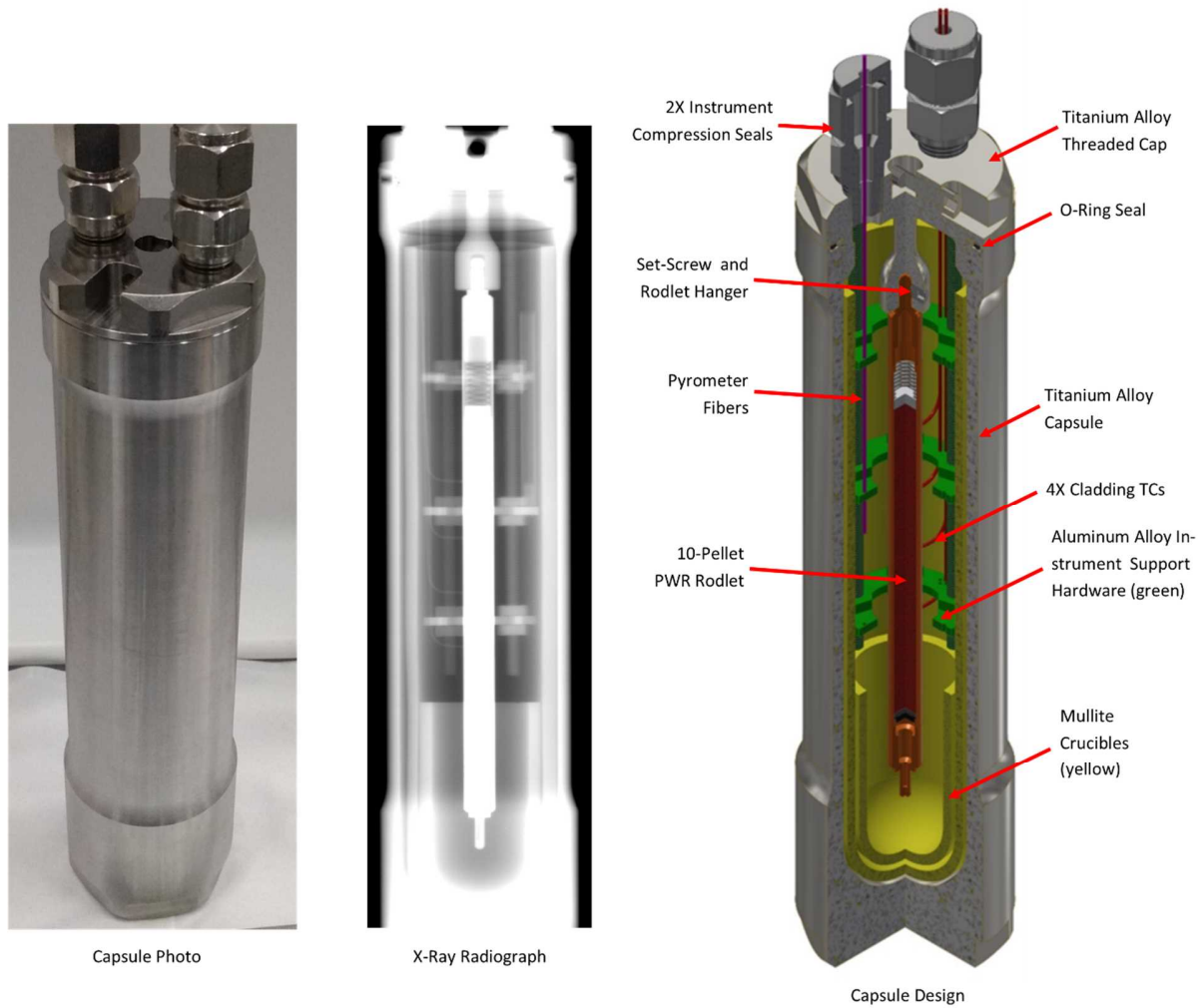


Figure 5: SETH Assembled Capsule Photograph (left), X-Ray Radiograph with Capsule Internals (middle), and Capsule Design Renderings (right)

III. Experimental Method for Determining Energy Coupling Data

During TREAT's most recent historic experiments the most common practice for determining core-to-specimen power coupling included radio-chemical evaluation of fissile specimens irradiated in mock experiment vehicles. Low level steady state runs (<120 kW core power) were performed on both fuel specimens and fission wires (typically in separate runs) to determine the core-to-specimen power coupling factors. A third irradiation, which was performed on fission wires only, employed the intended transient so that transient correction factors could be inferred by comparing steady state and transient fission wire irradiations. The need for a transient correction factor was clearly seen in these empirical results [4], but the exact physical causes remained both complicated and elusive, likely arising from the effects of control rod placement and transient rod motion on spatial neutron distribution, including their effect on reactor power instrumentation, as well as spectral neutron shift during core transient heating. The product of these factors and the core's transient power shape were needed to predict safety-case performance of high-energy final transient tests as well as evaluate the research outcomes of the test.

While this dosimeter-based method was an established historic approach, much of the supporting expertise and infrastructure was no longer available upon TREAT's 2017 restart. Schedule implications of dosimeter evaluation logistics, and the scarcity of historic fission wire materials which were typically uncommon alloys having very dilute uranium concentration to prevent their melting during transient irradiations, lent to a different approach using in-situ calorimetry measurement strategies for these initial SETH tests. Unlike fissionable dosimeter tests which measured power coupling and transient correction factors separately, the calorimetric method essentially measured both at the same time. Hence the term Energy Coupling Factor (ECF) was used to describe the outcome of these experiments.

In the SETH calorimetry approach temperature measurements of the rodlet's cladding surfaces were to be correlated with thermal models of the experiment. This strategy was simulated prior to the experiment irradiations by parametrically scaling ECFs predicted by state point Monte Carlo neutronic models and providing the time dependent power history to finite element thermal models of the experiment. Reactor power histories were originally predicted by point kinetics methods for design purposes, and later by trial transients performed in TREAT using a neutronically-equivalent dummy SETH capsule in the MARCH system. These power histories, particularly for the initial calorimetry-focused transient shapes, were input to the thermal model in order to correlate cladding temperatures to ECFs as expressed in the following equations where y is the ECF in units of J/gUO₂-MJ and x is cladding temperature in °C [10]:

Insulated case (SETH-A) $y = 0.0040x - 0.2743$

Uninsulated case $y = 0.0046x - 0.4138$

The above equations represented peak cladding surface temperature independent of any measurement effects. TC-based measurements of transient-heated surfaces were expected to measure significantly lower than true cladding temperature due their thermal mass response time and cooling fin effect on the cladding area they are measuring.

The yet-to-be demonstrated non-contact pyrometer method was expected to be immune from the response time and fin effect problems in TCs. Prior to irradiation of the initial SETH capsules an optical fiber was connected to a multispectral pyrometer and exposed to transient irradiations in TREAT's core within a small tube where it would measure no significant temperature change in order to characterize neutron/gamma-induced effects in the fiber. These efforts showed that irradiation-induced fiber darkening effects were insignificant in transient exposures and that the light collected by the fiber optics in SETH will be dominated by the black body irradiation

compared to the radiation induced emission. Prior to first SETH irradiations the custom-designed pyrometer optical line, was calibrated in accordance with standard practices using a traceable black body furnace.

IV. Calorimetric Specimen Energy Coupling for Low Energy Transients

Three low power transients were executed with practically identical reactor operating parameters starting with SETH-A. The second capsule was irradiated with the same low-energy transient twice under the same conditions (SETH-B1 and SETH-B1-R2) to investigate different pyrometry data acquisition settings. All of these three irradiations were performed using small reactivity step insertions ($0.6\% \Delta k/k$) which yielded relatively slow pulse with low energy release, but adequate to cause a measurable temperature rise in the specimen and well within the expected instrument calibration/survival range. While TREAT pulses self-limit their energy release due to predictable feedback kinetics, a significant amount of energy is released long after the pulse apex in a relatively slow decay tail. In order to yield a more-definitive end to transient nuclear heating for simplified post-test calorimetry data interpretation, these transients were all terminated tens of seconds after initiation via transient rod reinsertion “clipping” to at a nominal 100 MJ core energy release. The reactor power data and cladding temperature gathered for these three tests is shown in Figure 6.

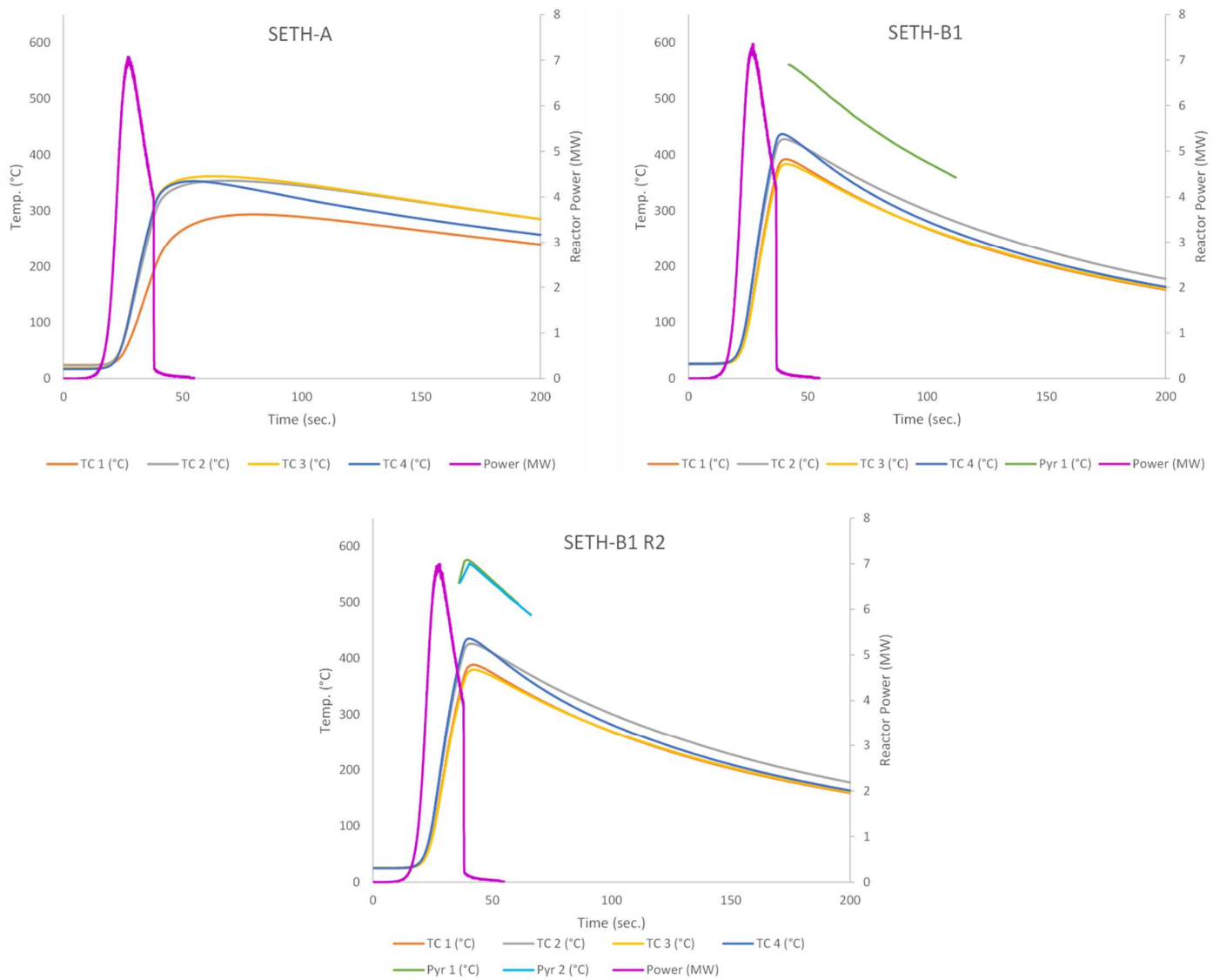


Figure 6: Cladding Temperature Data for Calibration SETH Tests

The temperature responses performed as expected in SETH-A, showing that the detached TC-1 produced both delayed and reduced peak temperatures, while the other TCs grouped together and gave confidence that all three remained attached. The more rapid post-transient temperature decay observed in the SETH-B1 irradiations performed as expected compared to the SETH-A insulated rodlet and the grounded junction TCs responded more quickly with higher ultimate

temperature measurements. The peak temperatures observed by the ungrounded TCs in SETH-B1 were slightly higher than those in SETH-A which was not expected due to absence of thermal insulation. As-run transient histories were virtually identical between these tests and the only major physical difference between the capsules was exchange of the silica thermal insulation for the aluminum instrument cage, both of which were predicted to be practically negligible in Monte Carlo neutronic models. These observations suggested that thermal resistances between the cladding, TC sheaths, and TC junctions were greater than expected so that heat transfer from the sheaths to the insulation in SETH-A were greater than originally anticipated.

Unlike the TCs, SETH's pyrometer system was not capable of providing measurements below 300 °C as a minimum amount of light emission was required to make temperature measurements. The pyrometer system also required several seconds of integration time in the low temperature range (~300-400 °C). Based on the relatively low temperature TC data observed in SETH-A, a large time step was selected for the initial pyrometer integration time in SETH-B1. Only one of the two optical fibers in SETH-B1 was connected to a pyrometer unit. During SETH-B1 the detector immediately saturated during the temperature rise. The pyrometer then began automatically reducing exposure time in each successive step until valid non-saturated measurements were obtained. As a result, the first valid pyrometer temperature data point was observed slightly after when the true peak occurred. For this reason, the SETH-B1 irradiation was repeated (SETH-B1-R2) with identical transient conditions, except the second fiber was also connected to a pyrometer unit and shorter initial light integration times were chosen. A peak cladding temperature as indicated by TCs and pyrometers were found to be 437 °C (TC-4) and 576 °C (Pyro-1), respectively. Post-test spectral data evaluation showed very good agreement

between the Pyro-1 data and Planck's law; giving temperature measurement accuracy within ± 14 °C ($\pm 2\%$).

All SETH temperature instruments and signal processing equipment were calibrated in accordance with standard practices before their use. Comparison of the instruments was also performed in a thermowell furnace in the TREAT facility so that TCs and pyrometer fibers could be placed in an isothermal environment at 400 °C with data acquisition through the same signal chains used in SETH irradiations. This effort demonstrated good agreement between TC and pyrometer measurements. Similarly, an electrically-heated out-of-pile mockup was also assembled to further investigate the situation. Care was taken to use representative zirconium alloy cladding, identical TCs and pyrometer equipment, and representative assembly procedures including use of the same TC welding equipment and assembly personnel. The resulting test was transient heated over a few minutes by a small cartridge heater forced into a tight fit within the mock cladding tube. At relevant temperature ranges in natural convection air this effort showed >100 °C disparity between TC and pyrometer measurements, and approximately 400 °C disparity in forced convection air; supporting the hypothesis that the TC fin effect and/or thermal resistance between cladding and TCs was greater than first predicted.

Despite its novelty in this application, it was ultimately determined that the pyrometer data was the most accurate, and in any case most conservative, data source for computing the ECF in order to permit higher energy irradiations. Using the ECF-temperature correlation described earlier, the peak cladding temperature observed by Pyro-1 in SETH-B1-R2 gave an ECF of 2.2 J/gUO₂MJ. While not a comprehensive treatment of potential uncertainties, the potential error on this computed ECF was estimated so that it could be considered in obtaining experiment safety approvals. This estimate was obtained by using the square root of the sum of the squares for a

±3.5% term (which had been estimated previously based on uncertainties in thermo-mechanical properties [10]), the pyrometer’s self-reported measurement uncertainty of ±2%, and a maximum heat loss term. The maximum heat loss term was estimated by comparing the difference between the rodlet under adiabatic conditions and the as-measured peak temperature as shown in the following equation and Table 1.

$$\Delta T = (mC_p)/E$$

Table 1: Uncertainty Estimate

	Density (g/cm ³)	C _p (J/g-K)*	R _{inner} (cm)	R _{outer} (cm)	Height (cm)	Mass (g)	J/K	ECF (J/gMJ)	Energy @ 100 MJ (J)	Adiabatic ΔT (K)	
UO ₂	10.96	0.289	0.000	0.413	10.16	59.6	17.2	2.2	13350	775	
Zry	6.49	0.358	0.418	0.475	10.16	10.6	3.8	-	-	-	
Rodlet						70.2	21.0	-	13350	635	
										Measured ΔT (K)	552
										Heat loss max error	15.1%
										Pyrometer uncertainty	2.0%
										Properties uncertainty	3.5%
										Root sum of the squares	15.7%

V. Observations from Higher Energy Tests

The ECF of 2.2 J/gUO₂MJ obtained from the previously-described tests, in conjunction with the conservatively-estimated +15.7% measurement uncertainty, was suitable to obtain experiment safety permission for transients requiring greater than 25% of the experiment’s containment capacity. As a result the remaining SETH irradiations were performed with increased step insertions resulting in much narrower pulses. The SETH-B capsule was irradiated for a third and final time with a 1.2% Δk/k step insertion (termed SETH-B2), and clipped to yield moderate energy releases where instrumentation was expected to survive handily. Pyro 1 observed the

highest temperature in SETH-B2 at 757 °C. The brief nature of the SETH-B2 pulse allowed for determination of the temperature dependent heat transfer coefficient for the rodlet in the SETH capsule from observation of the temperature decay curve and knowledge of the mass and heat capacity for the fuel pellets and cladding. A finite element heat transfer model was constructed of the rodlet using the temperature dependent heat transfer coefficient derived from SETH-B2 and standard temperature dependent models of UO₂ and Zircaloy heat capacity and thermal conductivity. The as-run power history from the SETH-B2 pulse was incorporated into this model and the ECF was parametrically adjusted until in good agreement with the observed pyrometer temperatures. These evaluations yielded an ECF of 2.0 J/gUO₂MJ. This value was lower than observed in previous tests, but the prompt critical nature of this pulse better represented the physics of the planned conditions for SETH-C through -E in terms of control rod positioning and reduced contribution from delayed neutrons and fission fragments depositing heat in the specimen after the prompt part of the transient. As a result, ECF values of 2.2 and 2.0 J/gUO₂MJ were used for subsequent tests in the cases of safety evaluation and best estimate programmatic predictions, respectively.

The SETH-C irradiation used the same step insertion as SETH-B2, but was clipped much later to yield markedly increased specimen temperatures. The more extreme temperatures in SETH-C appeared to cause erratic behavior in some of the TCs likely due to mechanical detachment, but the pyrometer responded stably with a measured peak temperature of 1378 °C. This temperature was in good agreement with pre-transient predictions obtained using an ECF 2.0 J/gUO₂MJ; giving increased confidence in the observed ECF.

The step insertion was increased to 1.7% $\Delta k/k$ for SETH-D and the clip timing was determined using an ECF of 2.0 J/gUO₂MJ with the objective to just barely achieve the zirconium's melting

temperature of 1850 °C for partial cladding melt. SETH-D's transient data showed that it exceeded the temperature calibration range for the cladding TCs while Pyro 2 measured a peak cladding temperature of 1938 °C. Posttest neutron radiography was performed on the SETH-D capsule in TREAT's neutron radiography stand and a separated rodlet was clearly observed. The separation of the rodlet explains the higher than expected cladding measurement since through this process the higher temperature fuel is exposed to the optical scene. While it is unlikely the pyrometer fibers had a direct view of the fuel, it is probable that the thermal emission from the fuel was collected into the fiber through one or more reflections inside of the capsule. The top pellet was observed to be suspended from un-melted cladding likely because the cladding surrounding it reached slightly lower temperatures due to axial conduction upward to unheated hardware in the upper rodlet. This observation, in addition to instrumentation readings, suggested that the test objective of partial cladding melt had been achieved; again increasing confidence in the ECF of 2.0 J/gUO₂MJ inferred from SETH-B2.

Finally, SETH-E was irradiated with the same step insertion as SETH-D, but clipped several seconds later so that a stronger fast neutron signal from the rodlet could be observed by TREAT's fast neutron fuel motion monitoring system during its motion downward. Measured peak cladding temperatures of 2113 °C, erratic behavior from temperature instrumentation, data from the fuel motion monitoring system, and observation of the entire pellet stack displaced downward in posttest neutron radiography all confirmed that the rodlet's cladding was largely disrupted by melting during the transient. Cladding temperature data and neutron radiographs for these higher energy SETH tests can be seen in Figure 7 and Figure 8, respectively.

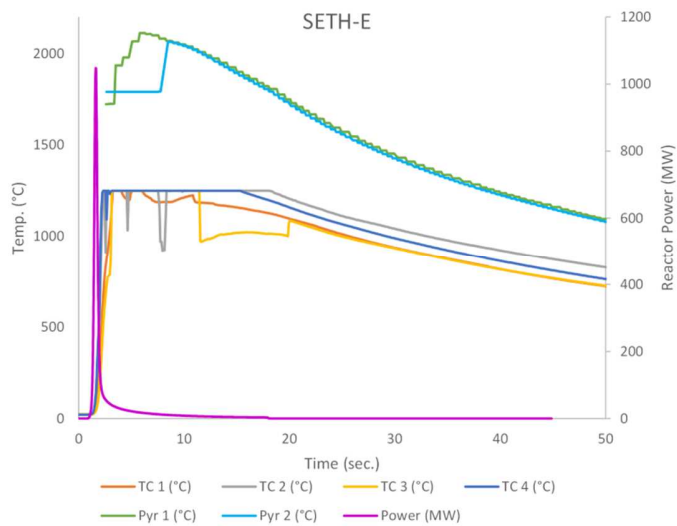
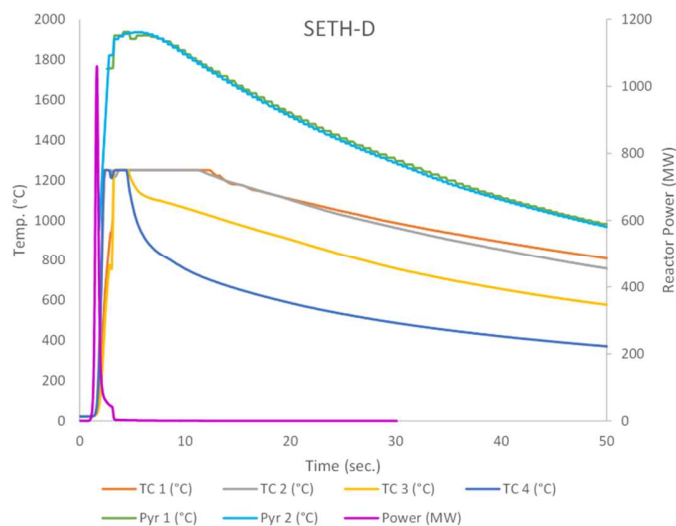
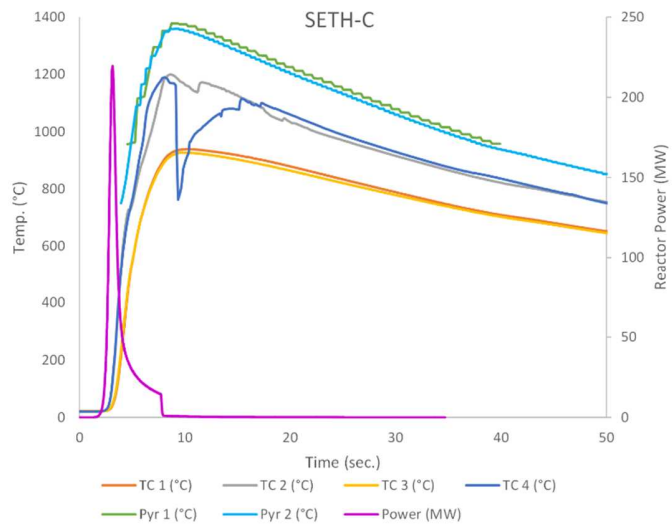
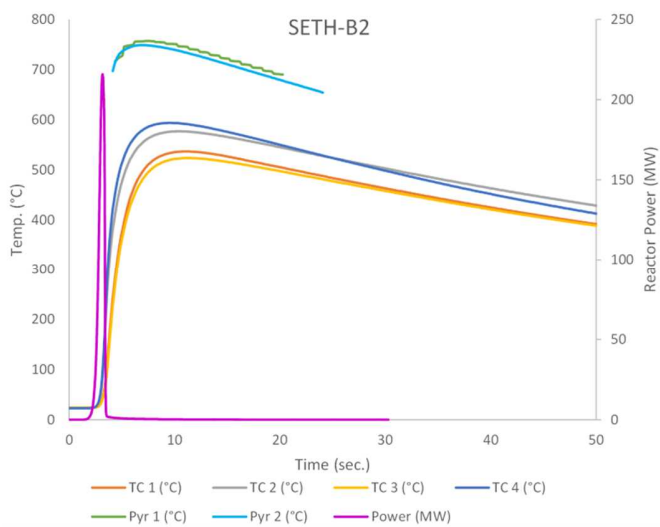


Figure 7: Cladding Temperature Data for Higher Energy SETH Tests

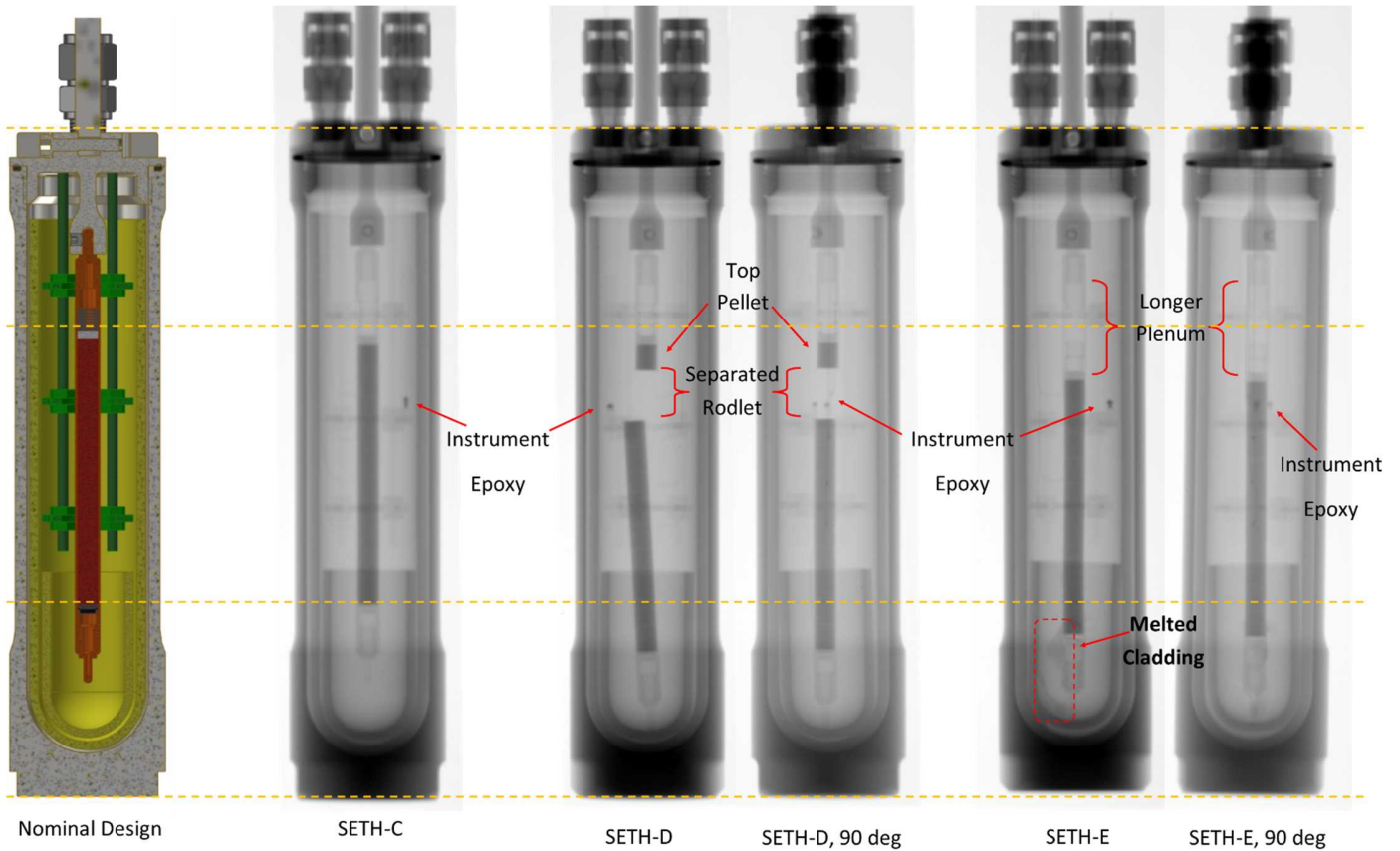


Figure 8: Comparison of Higher Energy SETH Tests, Post Transient Neutron Radiographs

VI. Transient Power and Flux History

While TREAT’s unique air-cooled design offers unparalleled access for instrumentation and experiments, it does pose some unique challenges in high certainty calibration of reactor power instrumentation by heat balance method. TREAT’s primary power instruments are ion chambers placed outside the graphite reflector in the concrete shielding where their measurements can also be influenced by control rod positions and transient rod motions. These considerations are important in any effort which aims to reconcile power coupling measurement with neutronic code calculations [11]. Accordingly, reactor power, core energy, and ECF data reported herein are considered to be “as-indicated” which, so long as reactor power instruments are not reconfigured

during a test campaign, is a suitable philosophy to enable one to progress from calibration measurements to final transients. However, to aid in the overall understanding of and ability to predict these behaviors, specifically as it pertains to neutron flux near the experiment position, specially-designed prompt response Self Powered Neutron Detectors (SPNDs) were also included in TREAT's core during the SETH irradiations as a complimentary data source.

These SPNDs were calibrated and used in TREAT to measured flux historically [12] and, due to occasional use in another low power critical reactor facility at the Idaho National Laboratory, had been retained in storage for TREAT's many years of inactivity. The SPNDs were connected to modern electrometers and placed in the small coolant channel locations formed between corner chamfers of adjacent fuel assemblies in TREAT's core. Data was gathered from a hafnium emitter SPND in position L-10-3 during SETH-A and -B1, position R-10-4 during SETH-B1 R2, and position L-10-4 during SETH-B2. Data was gathered from a gadolinium emitter SPND in position R-10-1 during SETH-B2 through -E. These data sets were converted to neutron flux in accordance with the historic method and generally agreed well with transient shapes from reactor power instrumentation as shown in Figure 10 and Figure 11.

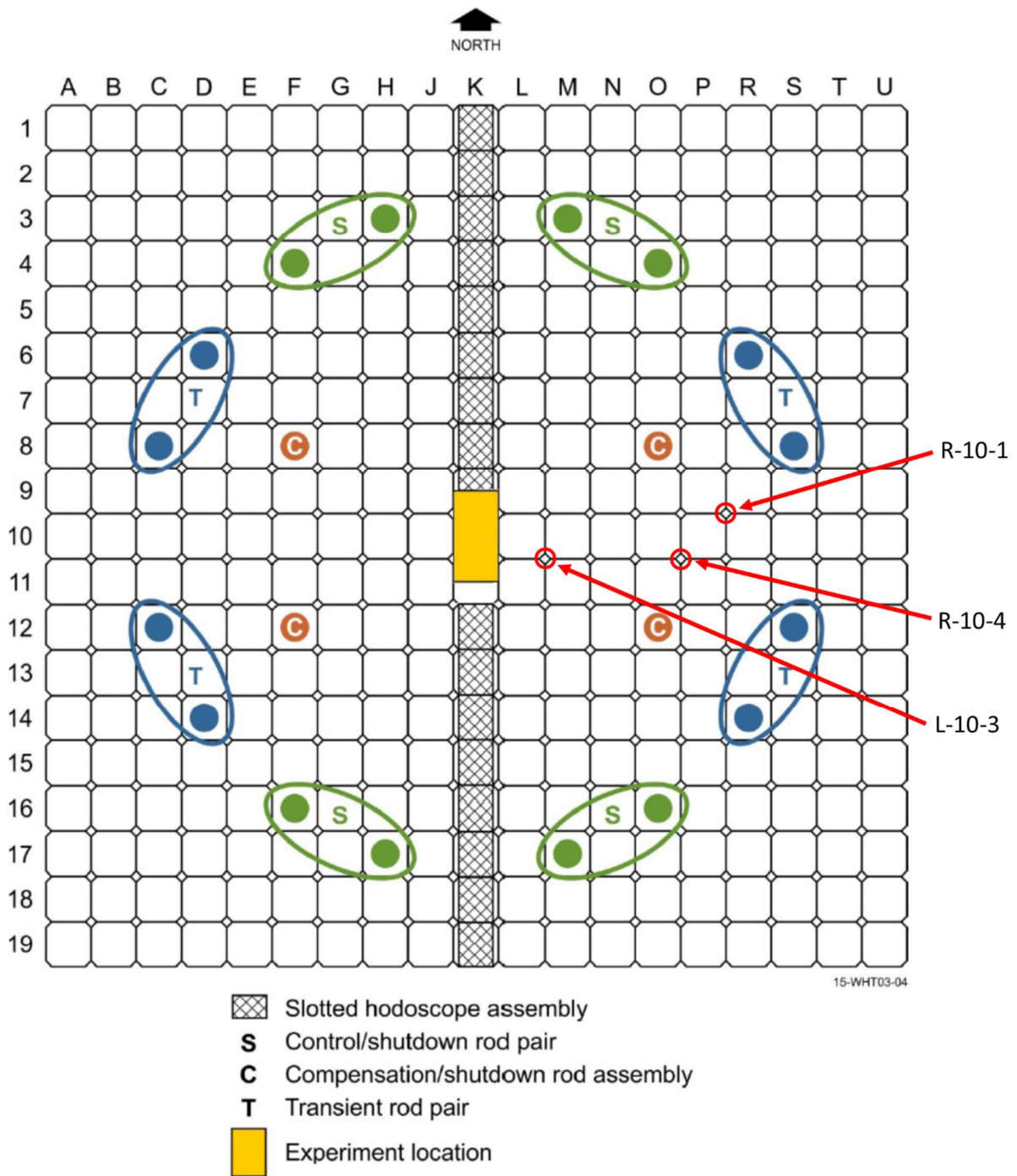


Figure 9: SPND Positions

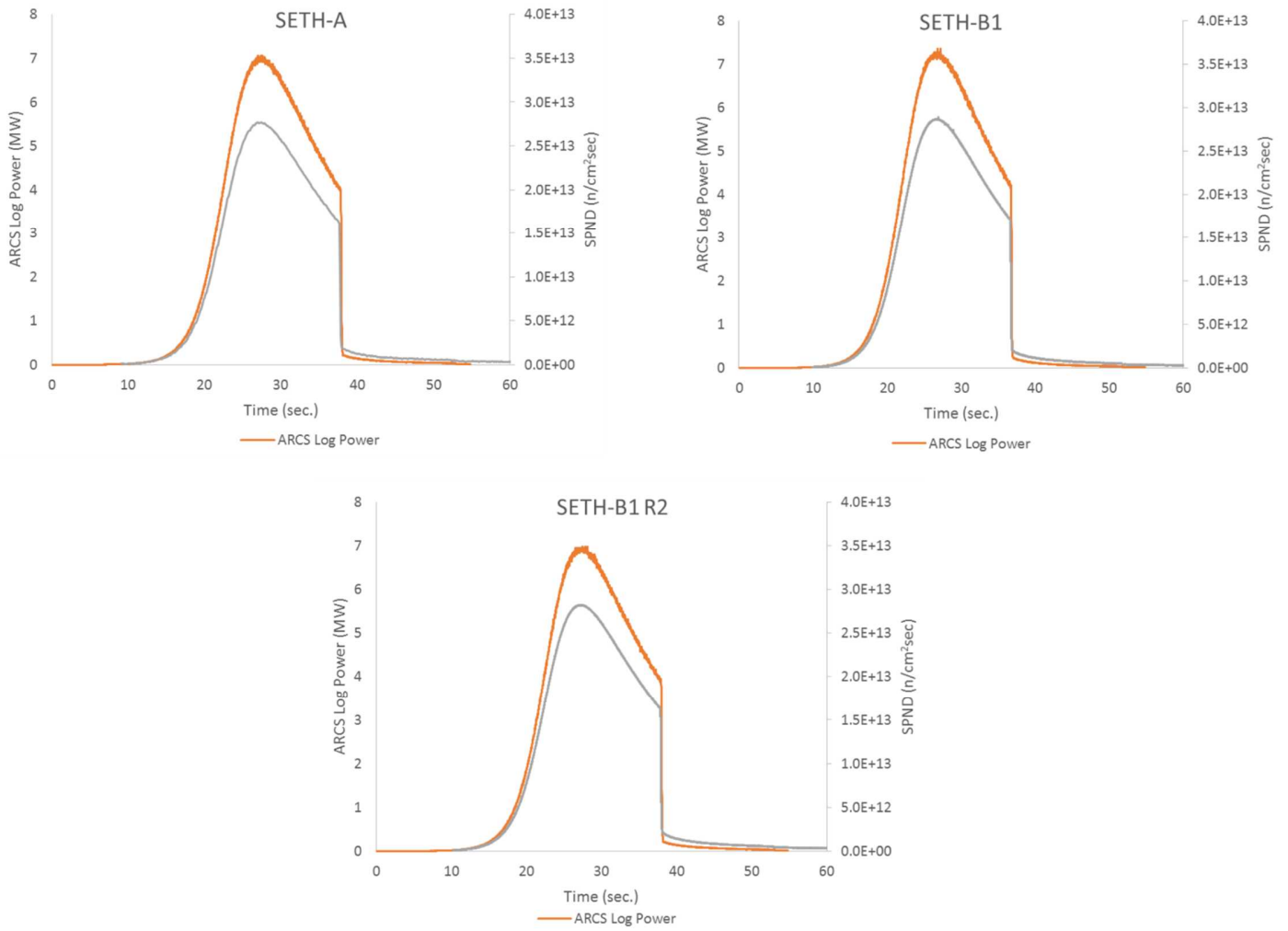


Figure 10: Reactor Power Instrumentation and SPND Flux for the Calibration SETH Tests

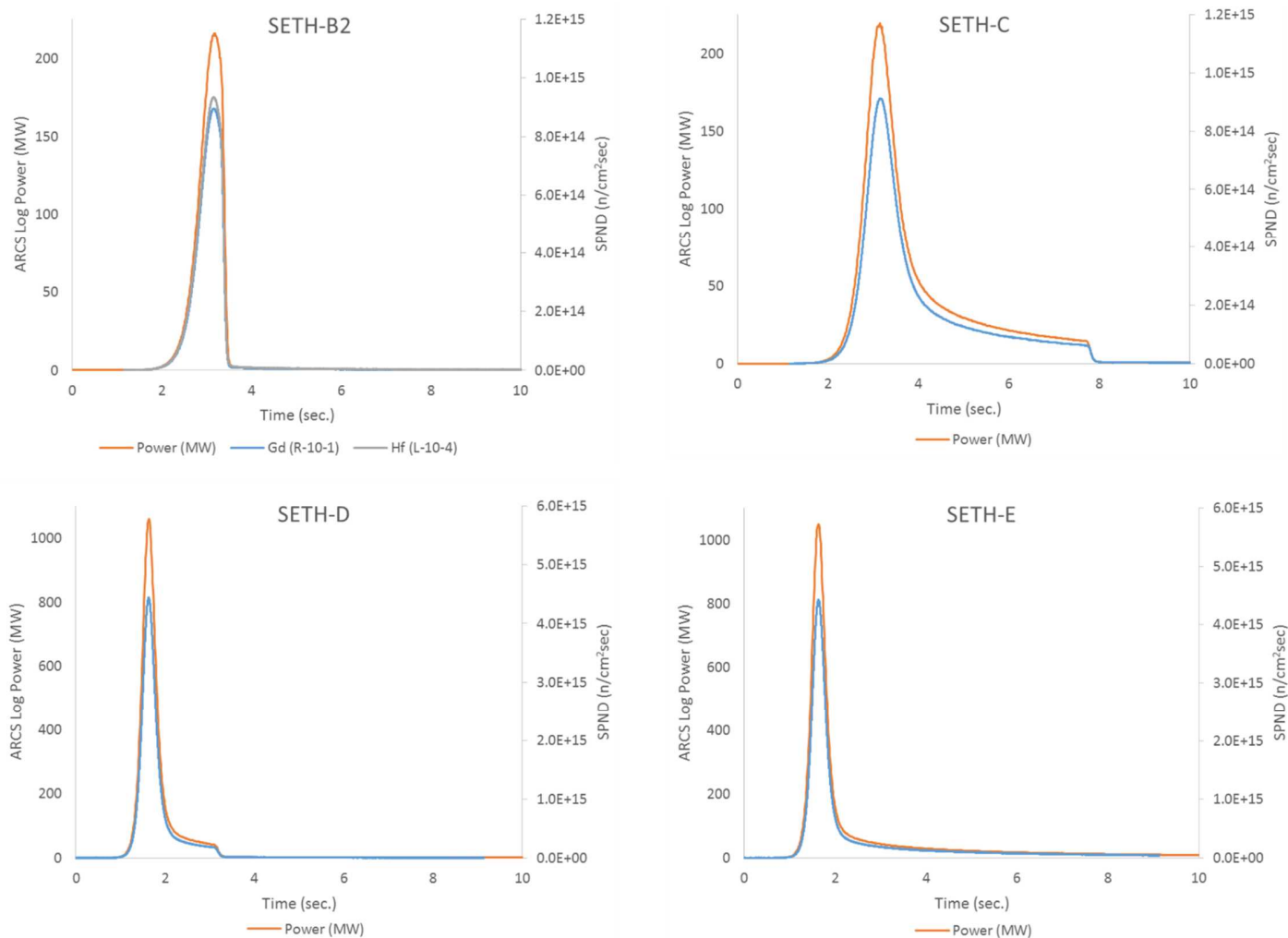


Figure 11: Reactor Power Instrumentation and SPND Flux for the Higher Energy SETH Tests

VII. Comparison to Gamma Spectroscopy

The SETH-A capsule was shipped for post irradiation disassembly and examination after its irradiation. The rodlet was characterized for gamma emission using a high purity germanium detector. Monte Carlo calculations were employed to correct for self-attenuation in the rodlet so that the gamma energy peaks for a few key fission product isotopes could be evaluated. These isotopes were correlated to fission events based on their fission yields and decay time following

irradiation. Using an assumed conversion of 182 MeV deposited per fission in the UO₂ and total reactor energy release of 101 MJ as indicated during SETH-A, these evaluations yielded an average power coupling factor of 2.1 J/gUO₂MJ with a total uncertainty of ±6%. The gamma spectroscopy results for SETH-A corroborated the in-situ calorimetric measurements and gave confidence in all the available energy coupling data. Gamma spectroscopy-based results for key fission product isotopes can be seen in Figure 12.

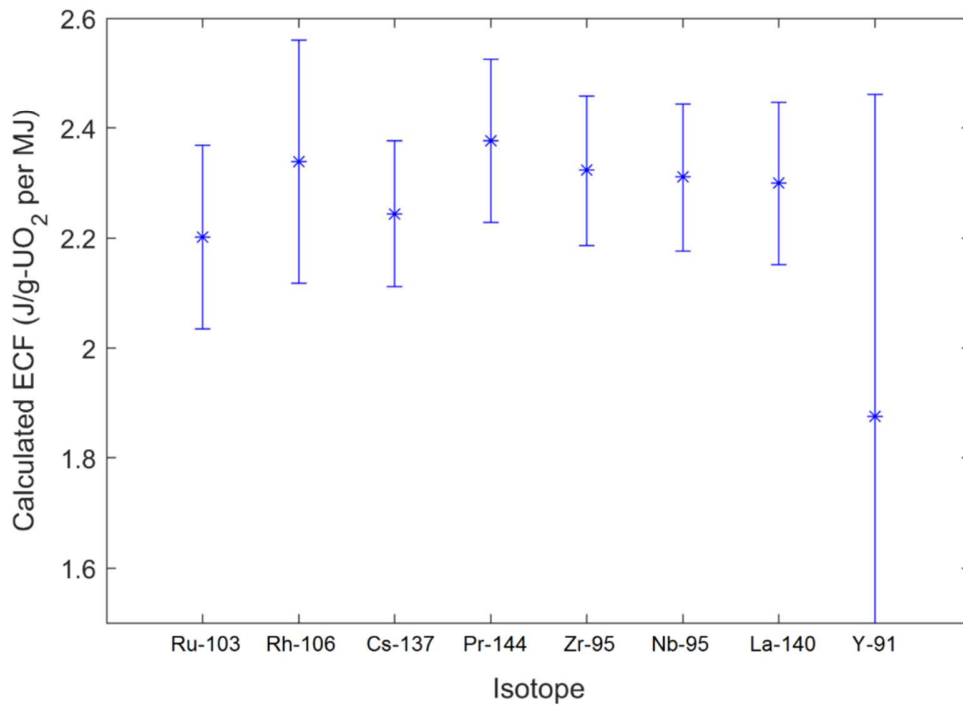
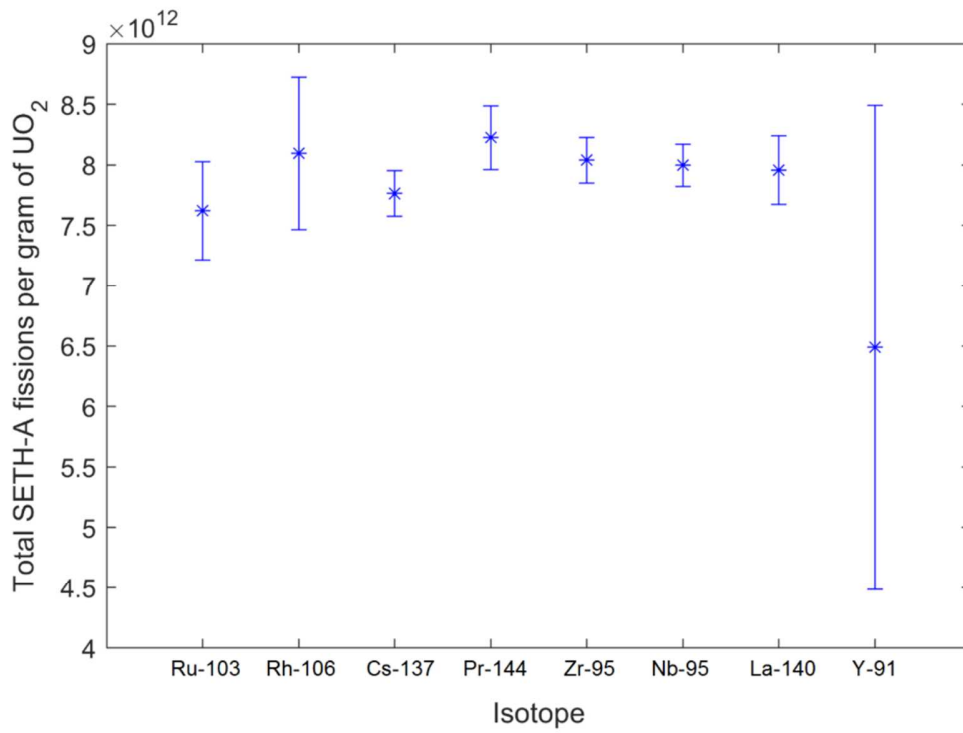


Figure 12: Fission Events and Calculated ECF from SETH-A Gamma Spectroscopy

VIII. Conclusions

TREAT's first year of experimental operations since 1994 were focused on demonstrating new LWR-relevant transient shapes representing RIA and LOCA. The successful outcome of these efforts paved the way for the first fuel experiments where a new irradiation vehicle system, associated instrumentation including novel application for pyrometry, and other support systems were successfully commissioned. Crucial core-to-specimen energy coupling for fresh 4.9% enriched UO₂ rodlets were measured by multiple methods with good corroboration giving a high confidence for ECF values between 2.0-2.2 J/gUO₂MJ in this experiment configuration. Demonstration of these multiple methods for ECF quantification provided model validation cases and measurement options to be in future experiment designs in TREAT. An overview of the key SETH test parameters and outcomes can be seen in Table 2.

Table 2: Overview Summary of Key Test Parameters

Test	Nominal Step Insertion (% $\Delta k/k$)	Total Reactor Energy (MJ)	Peak Reactor Power (MW)	Peak Cladding, Pyrometer ($^{\circ}\text{C}$)	ECF (J/gUO ₂ MJ)	Peak SPND Flux (n/cm ² s)	Specimen Energy Injection (J/g)	ECF Measurement Method
SETH-A	0.6	101	7.0	-	2.1	2.8e13	212	Gamma Spec
SETH-B1	0.6	101	7.3	561	2.2	2.9e13	222	Calorimetry (thermal modeling with pyrometer data)
SETH-B1 R2	0.6	101	7.0	576	2.2	2.8e13	222	
SETH-B2	1.2	143	214	757	2.0	9.3e14	286	
SETH-C	1.2	299	217	1378	2.0	9.1e14	598	Inferred by melting results and similarity to SETH-B2
SETH-D	1.7	501	1060	1938	2.0	4.4e15	1002	
SETH-E	1.7	656	1060	2113	2.0	4.4e15	1312	

IX. Acknowledgments

This work was supported through the Department of Energy Advanced Fuels Campaign under DOE Idaho Operations Office Contract DE-AC07-05ID14517. Accordingly, the U.S. Government retains and the publisher, by accepting the article for publication, acknowledges that the U.S.

Government retains a nonexclusive, paid-up, irrevocable, world-wide license to publish or reproduce the published form of this manuscript, or allow others to do so, for U.S. Government purposes.

X. Declaration of Interest

This information was prepared as an account of work sponsored by an agency of the U.S. Government. Neither the U.S. Government nor any agency thereof, nor any of their employees, makes any warranty, express or implied, or assumes any legal liability or responsibility for the accuracy, completeness, or usefulness of any information, apparatus, product, or process disclosed, or represents that its use would not infringe privately owned rights. References herein to any specific commercial product, process, or service by trade name, trademark, manufacturer, or otherwise, does not necessarily constitute or imply its endorsement, recommendation, or favoring by the U.S. Government or any agency thereof. The views and opinions of authors expressed herein do not necessarily state or reflect those of the U.S. Government or any agency thereof.

XI. References

1. G. A. FREUND, H. P. ISKENDARIAN, and D. OKRENT, "TREAT, A Pulsed Graphite-Moderated Reactor for Kinetics Experiments," Proc. 2nd United Nations Int. Conf. Peaceful Uses of Atomic Energy, Geneva, Switzerland, 1958, Vol. 10, p. 461 (1958).
2. THOMAS HOLSCHUH, NICOLAS WOOLSTENHULME, BENJAMIN BAKER, JOHN BESS, CLIFF DAVIS, and JAMES PARRY, "Transient Reactor Test Facility Advanced Transient Shapes", Nuclear Technology, Dec 2018.

3. N. E. WOOLSTENHULME, C. C. BAKER, J. D. BESS, C. B. DAVIS, C. M. HILL, G. K. HOUSLEY, C. B. JENSEN, N. D. JERRED, R. C. O'BRIEN, S. D. SNOW, and D. M. WACHS, "Capabilities Development for Transient Testing of Advanced Nuclear Fuels at TREAT," Proc. Int. Conf. Top Fuel 2016, Boise, Idaho, September 11-16, 2016, Track 3, p. 67, American Nuclear Society (2016).
4. W.R. ROBINSON, and T.H. BAUER, "The M8 Power Calibration Experiment (M8CAL)", Argonne National Laboratory Document ANL-IFR-232, May 1994.
5. GERALD KLOTZKIN, RICHARD W. SWANSON, PAUL HART, and L. J. HARRISON, "Time Dependence of Test Fuel Power Coupling During Transient Reactor Test Facility Irradiation Experiments", Nuclear Science and Engineering, 86:2, 206-218 (1984).
6. BENJAMIN BAKER, JAMES PARRY, THOMAS HOLSCHUH, CLIFF DAVIS, JAVIER ORTENSI, MARK DEHART, NICOLAS WOOLSTENHULME, DANIEL WACHS, and CONNIE HILL, "ATF Transient Prescription Tests in TREAT", INL Document INL/EXT-18-51416, Sep 2018.
7. JOHN D. BESS, NICOLAS E. WOOLSTENHULME, CLIFF B. DAVIS, LOUIS M. DUSANTER, CHARLES P. FOLSOM, JAMES R. PARRY, TATE H. SHORTHILL, and HAIHUA ZHAO, "Narrowing Transient Testing Pulse Widths to Enhance LWR RIA Experiment Design in the TREAT Facility," Annals of Nuclear Energy, 124 pp. 548-571, Oct 2018.
8. NICOLAS WOOLSTENHULME, CLINT BAKER, COLBY JENSEN, DANIEL CHAPMAN, DEVIN IMHOLTE, NATE OLDHAM, CONNIE HILL, and SPENCER

- SNOW, “Development of Irradiation Test Devices for Transient Testing,” Nuclear Technology, accepted manuscript Mar 2018.
9. JOHN D. BESS, NICOLAS E. WOOLSTENHULME, COLBY B. JENSEN, JAMES R. PARRY, and CONNIE M. HILL, "Nuclear Characterization of a General-Purpose Instrumentation and Materials Testing Location in TREAT," *Annals of Nuclear Energy*, 124 pp. 270-294, Oct 2018.
 10. D. CHAPMAN, “Safety and Programmatic Thermal Analysis for ATF-SETH in TREAT,” INL Document ECAR-4050, Rev 3, October 2018.
 11. MARK D. DEHART, BENJAMIN A. BAKER, and JAVIER ORTENSI, "Interpretation of Energy Deposition Data from Historical Operation of the Transient Test Facility (TREAT)." *Nuclear Engineering and Design* 322 (2017) 504–521, July 2017.
 12. G.R. IMEL, P.R. HART, “The Performance of Hafnium and Gadolinium Self Powered Neutron Detectors in the TREAT Reactor,” *Nuclear Instruments and Methods in Physics Research Section B: Beam Interactions with Materials and Atoms*, Volume 111, Issues 3–4, 1 May 1996, Pages 325-336.